ACS APPLIED MATERIALS & INTERFACES

Research Article

Cite This: ACS Appl. Mater. Interfaces 2020, 12, 2835−2841

www.acsami.org

High-Brightness and Color-Tunable $FAPbBr_3$ Perovskite Nanocrystals 2.0 Enable Ultrapure Green Luminescence for Achieving Recommendation 2020 Displays

Yanqing Zu,[†] Jun Xi,[‡,§] Lu Li,[†,∥] Jinfei Dai,[†] Shuangpeng Wang,[⊥] Feng Yun,[†] Bo Jiao,[†] Hua Dong,[†] Xun Hou,[†] and Zhaoxin Wu*[,†,#]

[†]Department of Electronic Science and Technology, School of Electronic and Information Engineering, Xi'an Jiaotong University, Xi'an 710049, Shaanxi, People's Republic of China

[‡]Global Frontier Center for Multiscale Energy Systems, Seoul National University, Seoul 08826, Korea

[§]Zernike Institute for Advanced Materials, University of Groningen, Nijenborgh 4, Groningen 9747 AG, The Netherlands

[∥]Ningbo Exciton Innovation Materials Research Institute Company Limited, Ningbo 315040, Zhejiang, People's Republic of China

[⊥]Joint Key Laboratory of the Ministry of Education, Institute of Applied Physics and Materials Engineering, University of Macau, Avenida da Universidade, Taipa 999078, Macau, China

[#]Collaborative Innovation Center of Extreme Optics, Shanxi University, Taiyuan 030006, Shanxi, People's Republic of China

S *Supporting Information*

ABSTRACT: To best catch human eyes in next-generation displays, the updated recommendation 2020 (Rec. 2020) standard has called for ultrapure green emitters to be qualified with a narrow emission of 525−535 nm with a full width at half-maximum (fwhm) below 25 nm. However, it is still challenging to find an emitter which can simultaneously cover these two criteria. Instead of traditional II−VI group semiconductor quantum dots, perovskite nanocrystals (NCs) can render versatile emitting tunability to allow them access to the Rec. 2020 standard. Herein, to realize the critical window of Rec. 2020, we have proposed a scalable, room temperature synthesis route of formamidinium lead bromide ($FAPbBr_3$) NCs using a sole ligand of sulfobetaine-18 (SBE-18). The as-synthesized $FAPbBr_3$ NCs exhibit an ideal emission at 534 nm with an ultranarrow fwhm of 20.5 nm and a high photoluminescence quantum yield of 90.6%, overwhelming the $FAPbBr_3$ nanoplates capped with oleic acid/oleylamine (OA/OAM). Introducing these high quality NCs into backlight displays, an ultrapure green backlight which covers ≈85.7% of the Rec. 2020 standard in the CIE 1931 color space is achieved, signifying the "greenest" backlight till now. Thus, we can foresee perovskite NCs as the most potential candidates for next-generation displays.

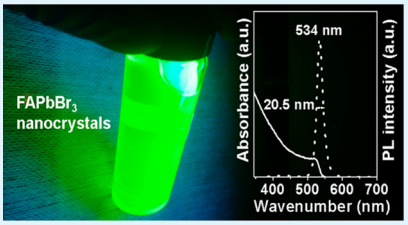

KEYWORDS: *formamidinium lead bromide nanocrystals, zwitterionic ligands, rec. 2020, ultrapure green luminescence*

1. INTRODUCTION

Conventional II−VI group inorganic semiconductor quantum dots have been considered as the most promising candidates to achieve the newly defined International Telecommunication Union (ITU) Recommendation BT 2020 (Rec. 2020) standard.[1] However, there still exist two drawbacks to hinder their commercialization: (i) a relatively broad full width at half-maximum (fwhm) of 25−35 nm;[2] (ii) the higher concentration cadmium usage beyond the maximum limit (100 ppm) in display equipment.[3] Therefore, exploring a cadmium-free material with ultranarrow fwhm remains challenging.

Recently, lead halide perovskites ($APbX_3$, where A is a metal cesium (Cs^+), methylammonium ($CH_3NH_3^+$; MA^+) and formamidinium ($CH(NH_2)_2^+$; FA^+) cation, and X is a Cl^-, Br^-, and I^- anion) have drawn extensive interests for backlight displays,[4−6] lasers,[7−9] photodetectors,[10,11] photovoltaics,[12−15] and light-emitting diodes (LEDs),[16−18] owing to not only their high photoluminescence quantum yield (PLQY) and narrow fwhm (<25 nm)[19−21] but also their lower cost and more simple synthesis.[22,23] Focusing on the most popular $MAPbBr_3$ and $CsPbBr_3$ nanocrystals (NCs), both of them generally possess a PL emission of <520 nm apart from $CsPbBr_3$ supercrystals,[24−28] far beyond the ultrapure green emission of 525−535 nm defined by the Rec. 2020 standard. To this end, the mixed halide perovskite ($MAPbBr_{3-x}I_x$ or $CsPbBr_{3-x}I_x$) NCs have been proposed to realize the desirable emission spectrum.[29−32] Unfortunately, the PLQY of such hybrid NCs tends to decrease,[33] significantly imposing the potential risk of the working stability. Besides, the iodine-ion incorporation will lead to the spontaneous phase separation under durable operation.[34,35]

Nowadays, it has been demonstrated that $FAPbBr_3$ with a smaller band gap than $MAPbBr_3$ and $CsPbBr_3$ can ideally reach the strict standard after being finely tuned.[36−38] For example,

Received: October 7, 2019
Accepted: December 23, 2019
Published: December 23, 2019

DOI: 10.1021/acsami.9b18140
ACS Appl. Mater. Interfaces 2020, 12, 2835−2841

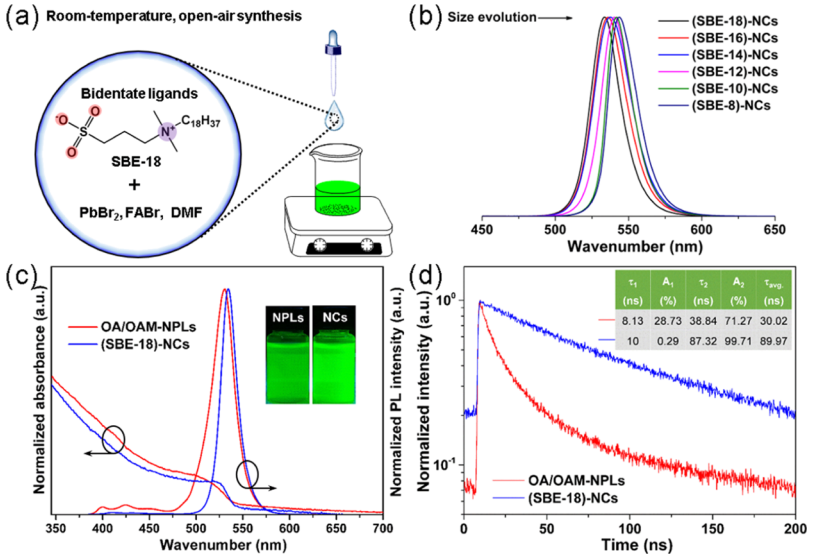

Figure 1. (a) Schematic illustration of the synthesis process of $FAPbBr_3$ NCs. (b) PL spectra of $FAPbBr_3$ NCs prepared with different carbon chain ligands. (c) UV−vis absorption and PL spectra of (SBE-18)-capped $FAPbBr_3$ NCs and OA/OAM-capped $FAPbBr_3$ NPLs, and the inset showing their colloidal solutions under 365 nm UV light. (d) Time-resolved photoluminescence lifetimes (TRPL) for (SBE-18)-capped NCs and OA/OAM-capped NPLs, and the inset showing their PL lifetimes.

Shih et al. reported ultrapure green LEDs at 531 nm PL emission using two-dimensional (2D) $FAPbBr_3$ nanoplates (NPLs).[2] Zeng et al. synthesized $FAPbBr_3$ NPLs with an emission of 525−535 nm through an ion-exchange-mediated self-assembly method.[39] Besides, Brabec et al. developed a ligand-assisted reprecipitation method to achieve $FAPbBr_3$ NPLs with 533 nm PL emission.[40] Obviously, all the abovementioned nano materials were prepared by using conventional ligands such as oleamine/acetic acid and octylamine/oleic acid. Nevertheless, there is a complicated protonation and deprotonation process between these coupled ligands, eventually leading to the poor stability.[41−46] Notably, recent reports have shown that zwitterion-capped $CsPbBr_3$ NCs possess a better stability and higher concentrated colloids than those of NCs capped by conventional ligands.[47,48] Therefore, the zwitterionic ligands could offer the feasibility to substitute the conventional ligands.

In this work, we synthesize colloidal 2D $FAPbBr_3$ NCs at room temperature in open air using a sole ligand of sulfobetaine-18 (SBE-18), which readily realize a desirable 534 nm emission with high color purity (fwhm ≈ 20.5 nm) and a high PLQY of up to 90.6%. As a downconverter, the (SBE-18)-capped $FAPbBr_3$ NCs enable the realization of an ultrapure green backlight with ∼85.7% Rec. 2020 coverage in the CIE 1931 color space, to the best of our knowledge, representing the "greenest" backlight till now.

2. EXPERIMENTAL SECTION

2.1. Chemicals. $PbBr_2$ (99.999%) and formamidinium bromide (FABr, 99.99%) were purchased from Alfa Aesar, and sulfobetaine 8 (SBE-8) (98%), sulfobetaine 10 (SBE-10) (98%), sulfobetaine 12 (SBE-12) (98%), 3-(*N*,*N*-dimethylmyristylammonio)-propanesulfonate (SBE-14) (98%), 3-(*N*,*N*-dimethylpalmitylammonio)propanesulfonate (SBE-16) (98%), 3-(*N*,*N*-dimethyloctadecylammonio)-propanesulfonate (sulfobetaine-18, SBE-18) (97%), and dichloromethane (≥99.8%) were purchased from Aladdin. Oleic acid (OA, 97%), oleylamine (OAM, 80−90%), *N*,*N*-Dimethylformamide (DMF, 99.9%), and toluene (>99%) were obtained from Sigma-Aldrich. All chemicals were used without further purification.

2.2. Synthesis of (SBE-18)-Capped $FAPbBr_3$ NCs. FABr (0.09 mmol) and $PbBr_2$ (0.1 mmol) were dissolved in 1 mL of DMF. Then, 0.05 mmol SBE-18 was added at 90 °C under vigorous stirring until completely dissolved. Subsequently, 100 μL of the hot precursor solution was injected into 3 mL of dichloromethane under vigorous stirring at room temperature in open air. The solution immediately turned yellow, and the reaction was finished within seconds. After the $FAPbBr_3$ crude solution was centrifuged at 6000 rpm for 2 min, the precipitates were dispersed in 4 mL of toluene. To be noted, all other SBE-based ligands maintain the same concentration of 0.05 mmol as SBE-18. For comparative investigation, $FAPbBr_3$ NPLs capped by OA/OAM ligands were obtained as the same as the synthesis step of $FAPbBr_3$ NCs capped by SBE-18, except for replacing with 0.05 mmol SBE-18 with 200 μL of OA and 40 μL of OAM without heating.

2.3. Fabrication of WLEDs. The fabrication process of the white LED (WLED) device is as follows: the red-emitting $K_2SiF_6:Mn^{4+}$ phosphors blended with poly(dimethylsiloxane) (PDMS) were directly dropped onto the blue-emitting GaN chip. Subsequently, the ultrapure green $FAPbBr_3$ NCs and PDMS mixture slurry were dropped. Finally, the obtained films were solidified in a vacuum drying oven, forming a downconversion layer.

2.4. Characterization. Powder X-ray diffraction (XRD) was performed with a X-ray diffractometer (D/MAX-2400, Rigaku, Japan) with Cu Kα radiation (λ = 1.54178 Å). X-ray photoelectron spectroscopy (XPS) spectra of the as-prepared samples were measured on a Thermo Fisher ESCALAB Xi$^+$. Transmission electron microscopy (TEM) images were collected on JEM-2100F (JEOL, Japan). Proton nuclear magnetic resonance spectroscopy (^{1}HNMR) was performed by employing a 400 MHz NMR (Bruker, CH). UV−vis absorption spectra were recorded with a Cary 5 spectrophotometer. FLS 920 spectrometer from Edinburgh Instruments was used to test the PLQY and photoluminescence lifetime. The electroluminescence (EL) spectrum, CIE color coordinates, and luminous efficiency of the fabricated devices were measured by using ATA-500 equipped with an integrating sphere.

3. RESULTS AND DISCUSSION

Colloidal 2D $FAPbBr_3$ NCs were synthesized via a modified ligand-assisted reprecipitation method at room temperature in open air,[40] whose schematic illustration is depicted in Figure 1a. The hybrid $FAPbBr_3$ NCs exhibit the enhanced PLQY and blue-shifted PL emission as the length of the carbon chain of

DOI: 10.1021/acsami.9b18140
ACS Appl. Mater. Interfaces 2020, 12, 2835−2841

ligands increases (Figure 1b), indicating the smaller size formation of NCs with a reduced nonradiative recombination center.[28,33] The short carbon chain of SBE-8 ligands, however, leads to the insufficient passivation and low PLQY (55.9%) of $FAPbBr_3$ NCs. When the carbon chain increased to 21, that is, SBE-18 ligands, the highest PLQY (90.6%) of NCs was achieved, and its optimal dosage was also obtained and shown in Figure S1. Figure S2 shows the crystal structure of (SBE-18)-capped $FAPbBr_3$ NCs, where both the functional amino and sulfonate groups of the ligands strongly bind to the surface cations and anions simultaneously. Figure 1c shows the PL and UV−vis absorption spectra of $FAPbBr_3$ capped by SBE-18 and OA/OAM ligands. The (SBE-18)-capped NCs exhibit the PLQY of 90.6%, much better than the PLQY value (83.2%) of OA/OAM-capped NPLs. In addition, the (SBE-18)-capped $FAPbBr_3$ NCs possess higher color purity (fwhm ≈ 20.5 nm) than OA/OAM-capped $FAPbBr_3$ NPLs (fwhm ≈ 24 nm). To be noted, the (OA + OAM)-capped $FAPbBr_3$ nanocubes could be also achieved, and they exhibited a PL peak exceeding 533 nm,[40] far from the ultrapure emission peak defined by the Rec. 2020 standard. Therefore, we study the ligand effect on $FAPbBr_3$ with different nanostructures. To the best of our knowledge, the highest PLQY and narrowest fwhm of $FAPbBr_3$ in this work have joined the leading league of $FAPbBr_3$ studies, as summarized in Table 1. TRPL of (SBE-18)-capped NCs and OA/OAM-capped NPLs are displayed in Figure 1d, and the curves are fitted by a biexponent decay function, where A and τ refer to the amplitude components and lifetimes, respectively. The average lifetime ($\tau_{ave.}$) is defined as $\tau_{ave.} = A_1 \cdot \tau_1 + A_2 \cdot \tau_2$. The lifetime ($\tau_{ave.}$) of (SBE-18)-capped NCs is 89.97 ns, which is nearly threefold longer than that of OA/OAM-capped NPLs (30.02 ns). This phenomenon shows the suppressed nonradiative recombination centers of NCs than those of NPLs (inset of Figure 1d). Notably, the PL decay curve of (SBE-18)-capped NCs is close to the single-exponent decay function, that is, achieving less trap of NCs and thereby an ultrahigh PLQY.[49]

Table 1. Summary of the PLQY, PL, and fwhm of $FAPbBr_3$ Studies

perovskite	PLQY (%)	PL (nm)	fwhm (nm)	date/reference
$FAPbBr_3$	90.6	534	20.5	this work
$FAPbBr_3$	88	532	21	2019[38]
$FAPbBr_3$	74	531.8	24.8	2018[39]
$FAPbBr_3$	76	518	20	2018[4]
$FAPbBr_3$	88	531	21.8	2017[2]
$FAPbBr_3$	85	533		2017[40]
$FAPbBr_3$	72	528	27	2017[33]
$FAPbBr_3$	85	530	22	2016[37]
$FAPbBr_3$	60	530	22.5	2016[36]

To confirm whether SBE-18 and OA/OAM ligands anchored on the perovskite surface and study how they affected the morphological and structural characteristic, TEM, XRD, XPS, and proton nuclear magnetic resonance spectroscopy (^{1}HNMR) were performed. Figure 2a−b shows the TEM images of OA/OAM-capped NPLs and (SBE-18)-capped NCs. The platelet-like morphology of OA/OAM-capped NPLs has an average lateral size and thickness of 22.3 and 2.5 nm, respectively. In parallel, the cubic-shape morphology of (SBE-18)-capped NCs has an average lateral size and thickness of 35.7 and 6.3 nm, respectively. Considering $FAPbBr_3$ monolayers with a unit cell thickness of ∼0.6 nm, $n \approx 4$ and $n \approx 10$ are therefore determined for (SBE-18)-capped NCs and OA/OAM-capped NPLs, respectively. Figure 2c displays the XRD patterns for (SBE-18)-capped NCs and OA/OAM-capped NPLs, revealing the highly crystallized cubic perovskite phase in both samples. The existence of sulfonate groups on the (SBE-18)-capped NC surface is confirmed by S 2p traces and typical infrared vibration modes (Figure 2d). In contrast, the sulfur element did not appear on the surface of OA/OAM-capped NPLs. Figure 2e shows the ^{1}HNMR spectra, where we can find that α_2-CH_2 ^{1}H resonances appeared at 2.64 ppm in (SBE-18)-capped NCs. Because of the nonexistence of the protonation and deprotonation process of amino and sulfonate groups, these ligands are able to strongly anchor on NC surfaces. However, for OA/OAM-capped NPLs, the complicated protonation and deprotonation process will occur between highly dynamic OA/OAM ligands, proven by the

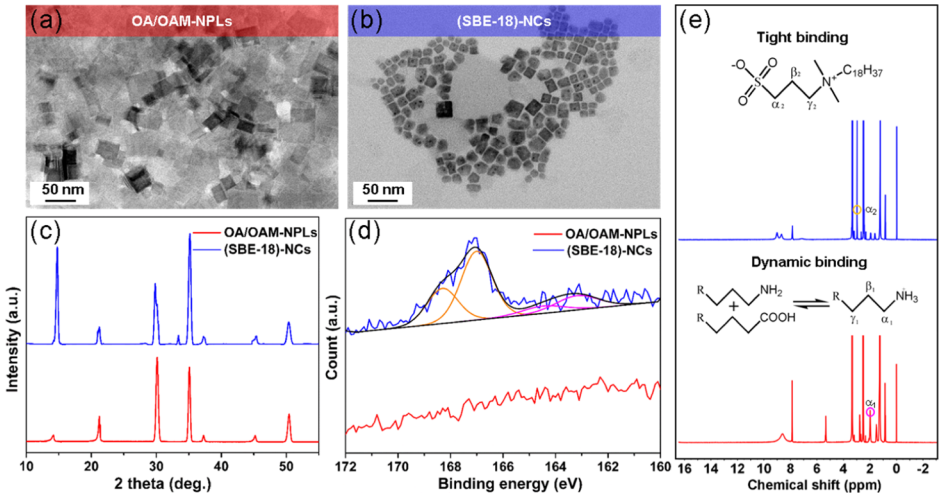

Figure 2. TEM images of (a) OA/OAM-capped $FAPbBr_3$ NPLs and (b) (SBE-18)-capped $FAPbBr_3$ NCs. (c) XRD patterns of (SBE-18)-capped NCs and OA/OAM-capped NPLs. (d) XPS spectra of S 2p for (SBE-18)-capped NCs and OA/OAM-capped NPLs. (e) ^{1}HNMR spectra of (SBE-18)-capped NCs and OA/OAM-capped NPLs.

DOI: 10.1021/acsami.9b18140
ACS Appl. Mater. Interfaces 2020, 12, 2835−2841

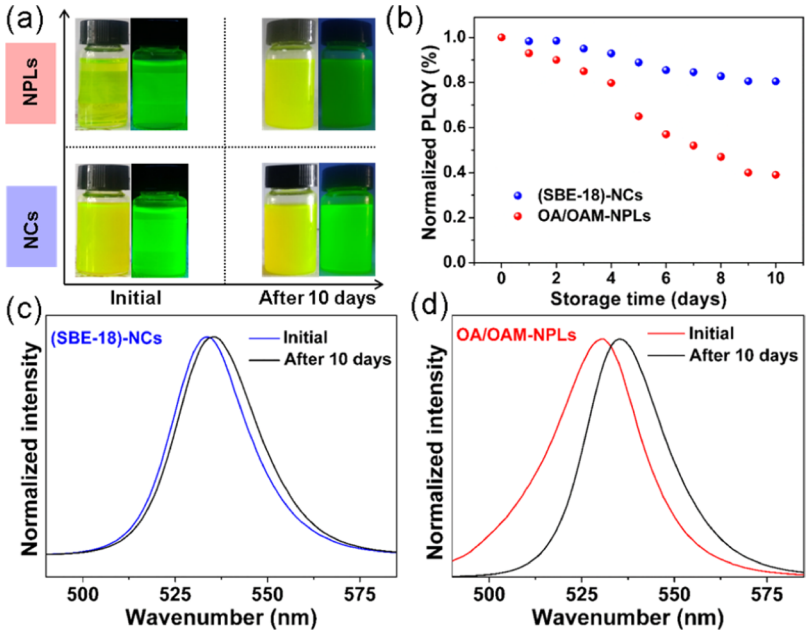

Figure 3. (a) Photographs of (SBE-18)-capped $FAPbBr_3$ NCs and OA/OAM-capped $FAPbBr_3$ NPLs before and after storage for 10 days under daylight and UV light. (b) PLQY changes for (SBE-18)-capped NCs and OA/OAM-capped NPLs after storage for 10 days under ambient conditions. (c) PL spectra of (SBE-18)-capped NCs before and after storage for 10 days. (d) PL spectra of OA/OAM-capped NPLs before and after storage for 10 days.

α_1-CH_2 ^1H signal at 12.16 ppm of $-NH_3^+$ in $OAmH^+$ coordinated with the surface Br atoms.[43]

As is known, the stability of colloidal perovskite NCs is critical to be overcome for practical applications. Interrogating the origins, there exists a weak binding state between ligands and NCs because of the ionic character of the perovskite lattice, which easily leads to the detachment of surface ligands and unstable NCs.[50] Besides, the perovskite inks are highly sensitive to the moisture and temperature, thus irreversibly deteriorating NCs. After storing for 10 days, the (SBE-18)-capped NCs could maintain a good dispersion as the same as the pristine solution. However, the OA/OAM-capped NPLs got turbid because of the formation of larger NPLs (Figure 3a). In addition, the (SBE-18)-capped NCs exhibit much higher brightness in comparison with OA/OAM-capped NPLs under UV light. More importantly, regarding (SBE-18)-capped NCs, the PL intensity dropped a little and the PL emission was almost unchanged after storing for 10 days (Figure 3b,c). However, regarding OA/OAM-capped NPLs, the PL intensity was merely retained at 48% of the initial value and an obvious red shift from 528 to 535 nm of the PL wavelength can be observed (Figure 3b,d). All the abovementioned results have indicated that the (SBE-18)-capped NCs possess higher stability over OA/OAM-capped NPLs. The origin of stability enhancement is as follows: the binding energy of sulfobetaine-18 ligands with NCs was computed to be ca. 40−45 kcal/mol, indicating good affinity of all of the ion pairs to the NC surface.[47] Besides, the colloidal stability of (SBE-18)-capped NCs is improved than conventional ligands capping NPLs because of the chelate effect.

The ligand-assisted reprecipitation method is performed at room temperature in open air instead of the most common hot-injection method requiring high temperature and an inert atmosphere.[51,52] Accordingly, this method not only can significantly save the cost but also is quite easy to be enlarged to the order of gram yield. Besides, the higher concentrated colloids are formed, when SBE-18 is used as surface ligands in replacement of conventional OA/OAM ligands. More importantly, the PL emission is able to be precisely tuned by using the sole ligand of SBE-18 instead of conventional OA/OAM ligands. As a verification, a 40-fold enlargement of the synthesis was implemented by increasing the amount of the precursor and synthetic solvent. Figure 4a shows the scale-up

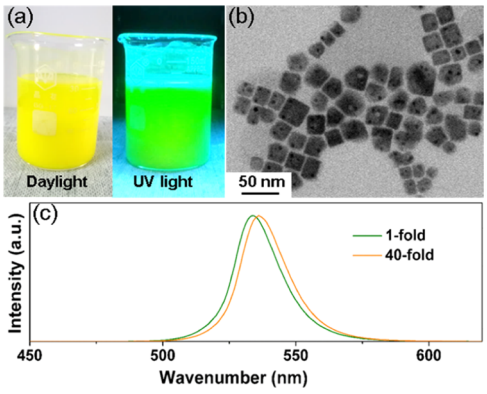

Figure 4. (a) Photographs of scaled-up 40-fold preparation of (SBE-18)-capped $FAPbBr_3$ NC colloidal solution under daylight and UV light. (b) TEM image of 40-fold synthesis for (SBE-18)-capped NCs. (c) PL spectra of (SBE-18)-capped NCs by a small-batch synthesis and a 40-fold enlarged synthesis.

to 40-fold of (SBE-18)-capped $FAPbBr_3$ colloidal solution under daylight and UV light (365 nm). The TEM image shows that there remains no obvious change in NC morphology when the synthesis was enlarged to 40-fold (Figure 4b). The PL spectra of the (SBE-18)-capped NCs by the enlargement preparation and small batch preparation are shown in Figure 4c, where a slightly red-shifted wavelength about 2 nm was observed and the fwhm was nearly unchanged. In addition, an

DOI: 10.1021/acsami.9b18140
ACS Appl. Mater. Interfaces 2020, 12, 2835−2841

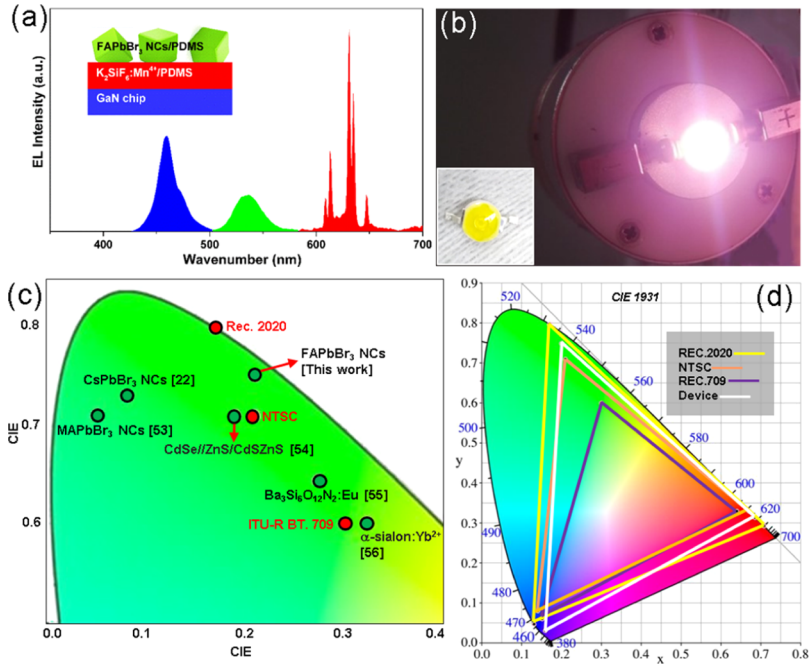

Figure 5. (a) EL spectrum of the WLED device. (b) Photograph of the WLED device operated at 2.6 V voltage. (c) Color coordinates of (SBE-18)-capped $FAPbBr_3$ NCs on the CIE 1931 color space compared with other green-emitting materials, including $CsPbBr_3$ NCs, $MAPbBr_3$, Cd-based quantum dots, $Ba_3Si_6O_{12}N_2$:Eu, and α-sialon:Yb^{2+}. (d) Color triangle of WLEDs on the CIE 1931 color space, together with the Rec. 2020 standards, National Television Standard Committee (NTSC), and Rec. BT 709 standard.

ultrahigh PLQY exceeding 80% was achieved. This facile scale-up production suggests that the synthesis method shows a great potential for industrialization available for future NC displays.

As an example of application in backlit displays, the WLEDdevices were fabricated by ultrapure green-emitting $FAPbBr_3$ NCs and commercially available red-emissive $K_2SiF_6:Mn^{4+}$ on the blue-emitting GaN chip. Figure 5a,b shows the EL spectrum of WLEDs and the photograph of the device operated at an applied voltage of 2.6 V, respectively. This as-fabricated device exhibited a color rendering index of 52 and a luminous efficiency of 50.9 lm/W. Encouragingly, for (SBE-18)-capped $FAPbBr_3$ NCs, an ultrapure green EL that locates at (0.20, 0.75) of the CIE coordinate was obtained (Figures 5c and S3), closer to the Rec. 2020 standard of (0.170, 0.797) compared with the advanced green-emitting materials such as $MAPbBr_3$,[53] $CsPbBr_3$ NCs,[22] Cd-based quantum dots,[54] $Ba_3Si_6O_{12}N_2$:Eu,[55] and α-sialon:Yb^{2+}.[56] The CIE chromaticity coordinate of the prototype device is (0.30, 0.25). In addition, a wide color gamut overlap of >85.7% Rec. 2020 standard, >114.7% NTSC standard, and >161.9% Rec. 709 standard of the WLEDs was achieved (Figure 5d), implying the bright future for next-generation displays.

4. CONCLUSIONS

In summary, high-performance colloidal 2D $FAPbBr_3$ NCs with bright and stable luminescence were synthesized on the basis of a sole zwitterionic ligand at room temperature in open air. Assemblying this ultrapure green-emitting material within backlight WLEDs, an ultrawide color gamut was achieved, which covered ≈85.7% of the Rec. 2020 standard in the CIE 1931 color space. This outstanding performance has joined the "greenest" backlight league ever reported. Our work not only sets a solid fundamental to obtain low-cost, large-scale, and high-quality $FAPbBr_3$ NCs but also demonstrates the great potential applications of perovskite NCs toward next-generation displays.

■ ASSOCIATED CONTENT

Supporting Information

The Supporting Information is available free of charge at https://pubs.acs.org/doi/10.1021/acsami.9b18140.

PL spectra of different molar ratios of SBE-18 for synthesis of $FAPbBr_3$ NCs; crystal structure of (SBE-18)-capped $FAPbBr_3$ NCs; XPS of Pb 4f and O 1s curves for (SBE-18)-capped $FAPbBr_3$ NCs and OA/OAM-capped $FAPbBr_3$ NPLs; photographs of the device fabricated by (SBE-18)-capped $FAPbBr_3$ NCs/PDMS on the blue-emitting GaN chip operated at 2.6 V voltage; selected-area electron diffraction for (SBE-18)-capped $FAPbBr_3$ NCs and OA/OAM-capped $FAPbBr_3$ NPLs; TEM images of OA/OAM-capped $FAPbBr_3$ NPLs and (SBE-18)-capped $FAPbBr_3$ NCs after storage for 10 days; and statistical Br/Pb atomic ratios for OA/OAM-capped $FAPbBr_3$ NPLs and (SBE-18)-capped $FAPbBr_3$ NCs calculated from XPS data (PDF)

(MP4)

(MP4)

■ AUTHOR INFORMATION

Corresponding Author

*E-mail: zhaoxinwu@mail.xjtu.edu.cn.

ORCID

Hua Dong: 0000-0001-9362-2236

Zhaoxin Wu: 0000-0003-2979-3051

Notes

The authors declare no competing financial interest.

DOI: 10.1021/acsami.9b18140
ACS Appl. Mater. Interfaces 2020, 12, 2835−2841

■ ACKNOWLEDGMENTS

This work was financially supported by the National Natural Science Foundation of China (grant no. 61875161, 11574248, and 61505161) and the National Key R&D Program of China (grant no. 2016YFB0400702). We expressed our gratitude for the help that Dr. X. J. Zhang and Dr. J. J. Zhang from the School of Science of Xi'an Jiaotong University provided in the TEM measurement and ^{1}HNMR, respectively, and we also thank Dr. Y. Wang from the Instrument Analysis Center of Xi'an Jiaotong University for her assistance in PLQY measurements.

■ REFERENCES

(1) Zhu, R.; Luo, Z.; Chen, H.; Dong, Y.; Wu, S.-T. Realizing Rec 2020 Color Gamut with Quantum Dot Displays. *Opt. Express* **2015**, *23*, 23680−23693.

(2) Kumar, S.; Jagielski, J.; Kallikounis, N.; Kim, Y.-H.; Wolf, C.; Jenny, F.; Tian, T.; Hofer, C. J.; Chiu, Y.-C.; Stark, W. J.; Lee, T.-W.; Shih, C.-J. Ultra-Pure Green Light Emitting Diodes Using Two-Dimensional Formamidinium Perovskites: Achieving Rec. 2020 Color Coordinates. *Nano Lett.* **2017**, *17*, 5277−5284.

(3) He, J.; Chen, H.; Chen, H.; Wang, Y.; Wu, S.-T.; Dong, Y. Hybrid downconverters with green perovskite-polymer composite films for wide color gamut displays. *Opt. Express* **2017**, *25*, 12915.

(4) Tong, Y.-L.; Zhang, Y.-W.; Ma, K.; Cheng, R.; Wang, F.; Chen, S. One-Step Synthesis of FA-Directing $FAPbBr_3$ PerovskiteNanocrystals toward High-Performance Display. *ACS Appl. Mater. Interfaces* **2018**, *10*, 31603−31609.

(5) Protesescu, L.; Yakunin, S.; Bodnarchuk, M. I.; Krieg, F.; Caputo, R.; Hendon, C. H.; Yang, R. X.; Walsh, A.; Kovalenko, M. V. Nanocrystals of Cesium Lead Halide Perovskites ($CsPbX_3$, X=Cl, Br, and I): Novel Optoelectronic Materials Showing Bright Emission with Wide Color Gamut. *Nano Lett.* **2015**, *15*, 3692−3696.

(6) Wang, H.-C.; Lin, S.-Y.; Tang, A.-C.; Singh, B. P.; Tong, H.-C.; Chen, C.-Y.; Lee, Y.-C.; Tsai, T.-L.; Liu, R.-S. Mesoporous Silica Particles Integrated with All-Inorganic $CsPbBr_3$ Perovskite Quantum-Dot Nanocomposites (MP-PQDs) with High Stability and Wide Color Gamut Used for Backlight Display. *Angew. Chem., Int. Ed.* **2016**, *55*, 7924−7929.

(7) Wang, L.; Meng, L.; Chen, L.; Huang, S.; Wu, X.; Dai, G.; Deng, L.; Han, J.; Zou, B.; Zhang, C.; Zhong, H. Ultralow-Threshold and Color-Tunable Continuous-Wave Lasing at Room-Temperature from In Situ Fabricated Perovskite Quantum Dots. *J. Phys. Chem. Lett.* **2019**, *10*, 3248−3253.

(8) Pan, J.; Sarmah, S. P.; Murali, B.; Dursun, I.; Peng, W.; Parida, M. R.; Liu, J.; Sinatra, L.; Alyami, N.; Zhao, C.; Alarousu, E.; Ng, T. K.; Ooi, B. S.; Bakr, O. M.; Mohammed, O. F. Air-Stable Surface-Passivated Perovskite Quantum Dots for Ultra-Robust, Single- and Two-Photon-Induced Amplified Spontaneous Emission. *J. Phys. Chem. Lett.* **2015**, *6*, 5027−5033.

(9) Veldhuis, S. A.; Tay, Y. K. E.; Bruno, A.; Dintakurti, S. S. H.; Bhaumik, S.; Muduli, S. K.; Li, M.; Mathews, N.; Sum, T. C.; Mhaisalkar, S. G. Benzyl Alcohol-Treated $CH_3NH_3PbBr_3$ Nanocrystals Exhibiting High Luminescence, Stability, and Ultralow Amplified Spontaneous Emission Thresholds. *Nano Lett.* **2017**, *17*, 7424−7432.

(10) Ahmed, G. H.; El-Demellawi, J. K.; Yin, J.; Pan, J.; Velusamy, D. B.; Hedhili, M. N.; Alarousu, E.; Bakr, O. M.; Alshareef, H. N.; Mohammed, O. F. Giant Photoluminescence Enhancement in $CsPbCl_3$ Perovskite Nanocrystals by Simultaneous Dual-Surface Passivation. *ACS Energy Lett.* **2018**, *3*, 2301−2307.

(11) Kwak, D.-H.; Lim, D.-H.; Ra, H.-S.; Ramasamy, P.; Lee, J.-S. High Performance Hybrid Graphene−$CsPbBr_{3-x}I_x$ Perovskite Nanocrystal Photodetector. *RSC Adv.* **2016**, *6*, 65252−65256.

(12) Akkerman, Q.; Gandini, M.; Di Stasio, F.; Rastogi, P.; Palazon, F.; Bertoni, G.; Ball, J.; Prato, M.; Petrozza, A.; Manna, L. Strongly Emissive Perovskite Nanocrystal Inks for High-Voltage Solar Cells. *Nat. Energy* **2016**, *2*, 16194.

(13) Wang, Y.; Dar, M.; Ono, L.; Zhang, T.; Kan, M.; Li, Y.; Zhang, L.; Wang, X.; Yang, Y.; Gao, X.; Qi, Y.; Grätzel, M.; Zhao, Y. Thermodynamically Stabilized β-$CsPbI_3$−Based Perovskite Solar Cells with Efficiencies >18%. *Science* **2019**, *365*, 591−595.

(14) Xi, J.; Xi, K.; Sadhanala, A.; Zhang, K. H. L.; Li, G.; Dong, H.; Lei, T.; Yuan, F.; Ran, C.; Jiao, B.; Coxon, P. R.; Harris, C. J.; Hou, X.; Kumar, R. V.; Wu, Z. Chemical Sintering Reduced Grain Boundary Defects for Stable Planar Perovskite Solar Cells. *Nano Energy* **2019**, *56*, 741−750.

(15) Dong, H.; Xi, J.; Zuo, L.; Li, J.; Yang, Y.; Wang, D.; Yu, Y.; Ma, L.; Ran, C.; Gao, W.; Jiao, B.; Xu, J.; Lei, T.; Wei, F.; Yuan, F.; Zhang, L.; Shi, Y.; Hou, X.; Wu, Z. Conjugated Molecules "Bridge": Functional Ligand toward Highly Efficient and Long-Term Stable Perovskite Solar Cell. *Adv. Funct. Mater.* **2019**, *29*, 1808119.

(16) Han, D.; Imran, M.; Zhang, M.; Chang, S.; Wu, X.-g.; Zhang, X.; Tang, J.; Wang, M.; Ali, S.; Li, X.; Yu, G.; Han, J.; Wang, L.; Zou, B.; Zhong, H. Efficient Light-Emitting Diodes Based on in Situ Fabricated $FAPbBr_3$ Nanocrystals: The Enhancing Role of the Ligand-Assisted Reprecipitation Process. *ACS Nano* **2018**, *12*, 8808−8816.

(17) Pan, J.; Shang, Y.; Yin, J.; De Bastiani, M.; Peng, W.; Dursun, I.; Sinatra, L.; El-Zohry, A. M.; Hedhili, M. N.; Emwas, A.-H.; Mohammed, O. F.; Ning, Z.; Bakr, O. M. Bidentate Ligand-Passivated $CsPbI_3$ Perovskite Nanocrystals for Stable Near-Unity Photoluminescence Quantum Yield and Efficient Red Light-Emitting Diodes. *J. Am. Chem. Soc.* **2018**, *140*, 562−565.

(18) Yang, K.; Li, F.; Liu, Y.; Xu, Z.; Li, Q.; Sun, K.; Qiu, L.; Zeng, Q.; Chen, Z.; Chen, W.; Lin, W.; Hu, H.; Guo, T. All-Solution-Processed Perovskite Quantum Dots Light-Emitting Diodes Based on the Solvent Engineering Strategy. *ACS Appl. Mater. Interfaces* **2018**, *10*, 27374−27380.

(19) Pan, J.; Quan, L. N.; Zhao, Y.; Peng, W.; Murali, B.; Sarmah, S. P.; Yuan, M.; Sinatra, L.; Alyami, N. M.; Liu, J.; Yassitepe, E.; Yang, Z.; Voznyy, O.; Comin, R.; Hedhili, M. N.; Mohammed, O. F.; Lu, Z. H.; Kim, D. H.; Sargent, E. H.; Bakr, O. M. Highly Efficient Perovskite-Quantum-Dot Light-Emitting Diodes by Surface Engineering. *Adv. Mater.* **2016**, *28*, 8718−8725.

(20) Li, Z.; Kong, L.; Huang, S.; Li, L. Highly Luminescent and Ultrastable $CsPbBr_3$ Perovskite Quantum Dots Incorporated into a Silica/Alumina Monolith. *Angew. Chem., Int. Ed.* **2017**, *56*, 8134−8138.

(21) Dutta, A.; Behera, R. K.; Pal, P.; Baitalik, S.; Pradhan, N. Near-Unity Photoluminescence Quantum Efficiency for All $CsPbX_3$ (X=Cl, Br, and I) Perovskite Nanocrystals: A Generic Synthesis Approach. *Angew. Chem., Int. Ed.* **2019**, *58*, 5552−5556.

(22) Song, J.; Li, J.; Xu, L.; Li, J.; Zhang, F.; Han, B.; Shan, Q.; Zeng, H. Room-Temperature Triple-Ligand Surface Engineering Synergistically Boosts Ink Stability, Recombination Dynamics, and Charge Injection toward EQE-11.6% Perovskite QLEDs. *Adv. Mater.* **2018**, *30*, 1800764.

(23) Zhang, Y.; Sun, R.; Ou, X.; Fu, K.; Chen, Q.; Ding, Y.; Xu, L.-J.; Liu, L.; Han, Y.; Malko, A. V.; Liu, X.; Yang, H.; Bakr, O. M.; Liu, H.; Mohammed, O. F. Metal Halide Perovskite Nanosheet for X-ray High-Resolution Scintillation Imaging Screens. *ACS Nano* **2019**, *13*, 2520−2525.

(24) Dai, J.; Xi, J.; Li, L.; Zhao, J.; Shi, Y.; Zhang, W.; Ran, C.; Jiao, B.; Hou, X.; Duan, X.; Wu, Z. Charge Transport between Coupling Colloidal Perovskite Quantum Dots Assisted by Functional Conjugated Ligands. *Angew. Chem., Int. Ed.* **2018**, *57*, 5754−5758.

(25) Huang, S.; Guo, M.; Tan, J.; Geng, Y.; Wu, J.; Tang, Y.; Su, C.; Lin, C. C.; Liang, Y. Novel Fluorescence Sensor Based on All-Inorganic Perovskite Quantum Dots Coated with Molecularly Imprinted Polymers for Highly Selective and Sensitive Detection of Omethoate. *ACS Appl. Mater. Interfaces* **2018**, *10*, 39056−39063.

(26) Liu, Y.; Xu, Q.; Chang, S.; Lv, Z.; Huang, S.; Jiang, F.; Zhang, X.; Yang, G.; Tong, X.; Hao, S.; Ren, Y. Brightly Luminescent and Color-Tunable Green-Violet-Emitting Halide Perovskite $CH_3NH_3PbBr_3$ Colloidal Quantum Dots: an Alternative to Lighting

DOI: 10.1021/acsami.9b18140
ACS Appl. Mater. Interfaces 2020, 12, 2835−2841

and Display Technology. *Phys. Chem. Chem. Phys.* **2018**, *20*, 19950−19957.
(27) Tong, Y.; Yao, E.-P.; Manzi, A.; Bladt, E.; Wang, K.; Döblinger, M.; Bals, S.; Müller-Buschbaum, P.; Urban, A. S.; Polavarapu, L.; Feldmann, J. Spontaneous Self-Assembly of Perovskite Nanocrystals into Electronically Coupled Supercrystals: Toward Filling the Green Gap. *Adv. Mater.* **2018**, *30*, 1801117.
(28) Zu, Y.; Dai, J.; Li, L.; Yuan, F.; Chen, X.; Feng, Z.; Li, K.; Song, X.; Yun, F.; Yu, Y.; Jiao, B.; Dong, H.; Hou, X.; Ju, M.; Wu, Z. Ultra-Stable $CsPbBr_3$ Nanocrystals with Near-Unity Photoluminescence Quantum Yield via Postsynthetic Surface Engineering. *J. Mater. Chem. A* **2019**, *7*, 26116−26122.
(29) Belarbi, E.; Vallés-Pelarda, M.; Clasen Hames, B.; Sanchez, R. S.; Maghraoui-Meherzi, E. M.; Mora-Seró, H.; Seró, I. Transformation of PbI_2, $PbBr_2$ and $PbCl_2$ Salts into $MAPbBr_3$ Perovskite by Halide Exchange as an Effective Method for Recombination Reduction. *Phys. Chem. Chem. Phys.* **2017**, *19*, 10913−10921.
(30) Hoffman, J. B.; Schleper, A. L.; Kamat, P. V. Transformation of Sintered $CsPbBr_3$ Nanocrystals to Cubic $CsPbI_3$ and Gradient $CsPbBr_xI_{3-x}$ through Halide Exchange. *J. Am. Chem. Soc.* **2016**, *138*, 8603−8611.
(31) Koscher, B. A.; Bronstein, N. D.; Olshansky, J. H.; Bekenstein, Y.; Alivisatos, A. P. Surface vs Diffusion Limited Mechanisms of Anion Exchange in $CsPbBr_3$ Nanocrystal Cubes Revealed through Kinetic Studies. *J. Am. Chem. Soc.* **2016**, *138*, 12065−12068.
(32) Nedelcu, G.; Protesescu, L.; Yakunin, S.; Bodnarchuk, M. I.; Grotevent, M. J.; Kovalenko, M. V. Fast Anion-Exchange in Highly Luminescent Nanocrystals of Cesium Lead Halide Perovskites ($CsPbX_3$, X = Cl, Br, I). *Nano Lett.* **2015**, *15*, 5635−5640.
(33) Kim, Y.-H.; Lee, G.-H.; Kim, Y.-T.; Wolf, C.; Yun, H. J.; Kwon, W.; Park, C. G.; Lee, T.-W. High Efficiency Perovskite Light-Emitting Diodes of Ligand-Engineered Colloidal Formamidinium Lead Bromide Nanoparticles. *Nano Energy* **2017**, *38*, 51−58.
(34) Draguta, S.; Sharia, O.; Yoon, S. J. Rationalizing the Light-Induced Phase Separation of Mixed Halide Organic-Inorganic Perovskites. *Nat. Commun.* **2017**, *8*, 200.
(35) Jiang, Y.; Qin, C.; Cui, M.; He, T.; Liu, K.; Huang, Y.; Luo, M.; Zhang, L.; Xu, H.; Li, S.; Wei, J.; Liu, Z.; Wang, H.; Kim, G.; Yuan, M. J.; Chen, J. Spectra Stable Blue Perovskite Light-Emitting Diodes. *Nat. Commun.* **2019**, *10*, 1868.
(36) Perumal, A.; Shendre, S.; Li, M.; Tay, Y. K.; Sharma, V. K.; Chen, S.; Wei, Z.; Liu, Q.; Gao, Y.; Buenconsejo, P. J.; Tan, S. T.; Gan, C. L.; Xiong, Q.; Sum, T. C.; Demir, H. V. High Brightness Formamidinium Lead Bromide Perovskite Nanocrystal Light Emitting Devices. *Sci. Rep.* **2016**, *6*, 36733.
(37) Protesescu, L.; Yakunin, S.; Bodnarchuk, M. I.; Bertolotti, F.; Masciocchi, N.; Guagliardi, A.; Kovalenko, M. V. Monodisperse Formamidinium Lead Bromide Nanocrystals ith Bright and Stable Green Photoluminescence. *J. Am. Chem. Soc.* **2016**, *138*, 14202−14205.
(38) Fang, H.; Deng, W.; Zhang, X.; Xu, X.; Zhang, M.; Jie, J.; Zhang, X. Few-Layer Formamidinium Lead Bromide Nanoplatelets for Ultrapure-Green and High-Efficiency Light-Emitting Diodes. *Nano Res.* **2019**, *12*, 171−176.
(39) Yu, D.; Cao, F.; Gao, Y.; Xiong, Y.; Zeng, H. Room-Temperature Ion-Exchange-Mediated Self-Assembly toward Formamidinium Perovskite Nanoplates with Finely Tunable, Ultrapure Green Emissions for Achieving Rec. 2020 Displays. *Adv. Funct. Mater.* **2018**, *28*, 1800248.
(40) Levchuk, I.; Osvet, A.; Tang, X.; Brandl, M.; Perea, J. D.; Hoegl, F.; Matt, G. J.; Hock, R.; Batentschuk, M.; Brabec, C. J. Brightly Luminescent and Color-Tunable Formamidinium Lead Halide Perovskite $FAPbX_3$ (X=Cl, Br, I) Colloidal Nanocrystals. *Nano Lett.* **2017**, *17*, 2765−2770.
(41) De Roo, J.; Ibáñez, M.; Geiregat, P.; Nedelcu, G.; Walravens, W.; Maes, J.; Martins, J. C.; Van Driessche, I.; Kovalenko, M. V.; Hens, Z. Highly Dynamic Ligand Binding and Light Absorption Coefficient of Cesium Lead Bromide Perovskite Nanocrystals. *ACS Nano* **2016**, *10*, 2071−2081.
(42) Smock, S. R.; Williams, T. J.; Brutchey, R. L. Quantifying the Thermodynamics of Ligand Binding to $CsPbBr_3$ Quantum Dots. *Angew. Chem., Int. Ed.* **2018**, *57*, 11711−11715.
(43) Zhong, Q.; Cao, M.; Xu, Y.; Li, P.; Zhang, Y.; Hu, H.; Yang, D.; Xu, Y.; Wang, L.; Li, Y.; Zhang, X.; Zhang, Q. L-Type Ligand-Assisted Acid-Free Synthesis of $CsPbBr_3$ Nanocrystals with Near-Unity Photoluminescence Quantum Yield and High Stability. *Nano Lett.* **2019**, *19*, 4151−4157.
(44) Tan, Y.; Zou, Y.; Wu, L.; Huang, Q.; Yang, D.; Chen, M.; Ban, M.; Wu, C.; Wu, T.; Bai, S.; Song, T.; Zhang, Q.; Sun, B. Highly Luminescent and Stable Perovskite Nanocrystals with Octylphosphonic Acid as a Ligand for Efficient Light-Emitting Diodes. *ACS Appl. Mater. Interfaces* **2018**, *10*, 3784−3792.
(45) Shynkarenko, Y.; Bodnarchuk, M. I.; Bernasconi, C.; Berezovska, Y.; Verteletskyi, V.; Ochsenbein, S. T.; Kovalenko, M. V. Direct Synthesis of Quaternary Alkylammonium-Capped Perovskite Nanocrystals for Efficient Blue and Green Light-Emitting Diodes. *ACS Energy Lett.* **2019**, *4*, 2703−2711.
(46) Xie, Q.; Wu, D.; Wang, X.; Li, Y.; Fang, F.; Wang, Z.; Ma, Y.; Su, M.; Peng, S.; Liu, H.; Wang, K.; Sun, X. W. Branched Capping Ligands Improve the Stability of Cesium Lead Halide (CsPbBr3) Perovskite Quantum Dots. *J. Mater. Chem. C* **2019**, *7*, 11251−11257.
(47) Krieg, F.; Ochsenbein, S. T.; Yakunin, S.; Ten Brinck, S.; Aellen, P.; Süess, A.; Clerc, B.; Guggisberg, D.; Nazarenko, O.; Shynkarenko, Y.; Kumar, S.; Shih, C.-J.; Infante, I.; Kovalenko, M. V. Colloidal $CsPbX_3$ (X = Cl, Br, I) Nanocrystals 2.0: Zwitterionic Capping Ligands for Improved Durability and Stability. *ACS Energy Lett.* **2018**, *3*, 641−646.
(48) Utzat, H.; Sun, W.; Kaplan, A.; Krieg, F.; Ginterseder, M.; Spokoyny, B.; Klein, N.; Shulenberger, K.; Perkinson, C.; Kovalenko, M.; Bawendi, M. Coherent Single-Photon Emission from Colloidal Lead Halide Perovskite Quantum Dots. *Science* **2019**, *363*, 1068.
(49) Bi, C.; Wang, S.; Kershaw, S. V.; Zheng, K.; Pullerits, T.; Gaponenko, S.; Tian, J.; Rogach, A. L. Spontaneous Self-Assembly of Cesium Lead Halide Perovskite Nanoplatelets into Cuboid Crystals with High Intensity Blue Emission. *Adv. Sci.* **2019**, *6*, 1900462.
(50) Yang, D.; Li, X.; Zhou, W.; Zhang, S.; Meng, C.; Wu, Y.; Wang, Y.; Zeng, H. $CsPbBr_3$ Quantum Dots 2.0: Benzenesulfonic Acid Equivalent Ligand Awakens Complete Purification. *Adv. Mater.* **2019**, *31*, 1900767.
(51) Huang, H.; Li, Y.; Tong, Y.; Yao, E.-P.; Feil, M. W.; Richter, A. F.; Döblinger, M.; Rogach, A. L.; Feldmann, J.; Polavarapu, L. Spontaneous Crystallization of Perovskite Nanocrystals in Nonpolar Organic Solvents: A Versatile Approach for their Shape-Controlled Synthesis. *Angew. Chem., Int. Ed.* **2019**, *58*, 16558−16562.
(52) Minh, D. N.; Kim, J.; Hyon, J.; Sim, J. H.; Sowlih, H. H.; Seo, C.; Nam, J.; Eom, S.; Suk, S.; Lee, S.; Kim, E.; Kang, Y. Room-Temperature Synthesis of Widely Tunable Formamidinium Lead Halide Perovskite Nanocrystals. *Chem. Mater.* **2017**, *29*, 5713−5719.
(53) Song, Y.-H.; Yoo, J. S.; Ji, E. K.; Lee, C. W.; Han, G. S.; Jung, H. S.; Yoon, D.-H. Design of Water Stable Green-Emitting $CH_3NH_3PbBr_3$ Perovskite Luminescence Materials with Encapsulation for Applications in Optoelectronic Device. *Chem. Eng. J.* **2016**, *306*, 791−795.
(54) Jang, E.; Jun, S.; Jang, H.; Lim, J.; Kim, B.; Kim, Y. White-Light-emitting Diodes with Quantum Dot Color Converters for Display Backlights. *Adv. Mater.* **2010**, *22*, 3076−3080.
(55) Mikami, M.; Shimooka, S.; Uheda, K.; Imura, H.; Kijima, N. New Green Phosphor $Ba_3Si_6O_{12}N_2$:Eu for White LED: Crystal Structure and Optical Properties. *Key Eng. Mater.* **2008**, *403*, 11−14.
(56) Xie, R.-J.; Hirosaki, N.; Kimura, N.; Sakuma, K.; Mitomo, M. 2-Phosphor-Converted White light-Emitting Diodes Using Oxynitride/Nitride Phosphors. *Appl. Phys. Lett.* **2007**, *90*, 191101.

DOI: 10.1021/acsami.9b18140
ACS Appl. Mater. Interfaces 2020, 12, 2835−2841